General and Comparative Endocrinology 301 (2021) 113657

Contents lists available at ScienceDirect

General and Comparative Endocrinology

journal homepage: www.elsevier.com/locate/ygcen

Research paper

Central prolactin receptor distribution and pSTAT5 activation patterns in breeding and non-breeding zebra finches (*Taeniopygia guttata*)

Kristina O. Smiley [a,*,1], Longying Dong [b], Selvakumar Ramakrishnan [c], Elizabeth Adkins-Regan [a,d]

[a] Department of Psychology, Cornell University, Ithaca, NY 14853, USA
[b] Department of Biomedical Sciences, Cornell University, Ithaca, NY 14853, USA
[c] Department of Biological Sciences, University of Wisconsin-Milwaukee, Milwaukee, WI 53211, USA
[d] Department of Neurobiology and Behavior, Cornell University, Ithaca, NY 14853, USA

ARTICLE INFO

Keywords:
Avian brain
Parental care
Prolactin
Prolactin receptor
pSTAT5
Songbird

ABSTRACT

The hormone prolactin has many diverse functions across taxa such as osmoregulation, metabolism, and reproductive behavior. In ring doves, central prolactin action is important for parental care and feeding behavior. However, there is a considerable lack of information on the distribution of the prolactin receptor (PRLR) in the avian CNS to test the hypothesis that prolactin mediates these and other functions in other birds. In order to advance this research, we collected brains from breeding and non-breeding zebra finches to map the PRLR distribution using immunohistochemistry. We found PRLRs are distributed widely across the brain, both in hypothalamic sites known to regulate parental care and feeding, but also in many non-hypothalamic sites, including the tectofugal visual pathway, song system regions, reward associated areas, and pallium. This raises the possibility that prolactin has other functions throughout the brain that are not necessarily related to feeding or parental care. In addition, we also stained brains for pSTAT5, a transcription factor which is expressed when the PRLR is activated and is used as a marker for PRLR activity. We found several notable differences in pSTAT5 activity due to the breeding state of the animal, in both directions, further supporting the hypothesis that prolactin has many diverse functions in the brain both within and outside times of breeding. Together, this study represents the first essential step to inform the design of causative studies which manipulate PRLR-expressing cells to test their role in a wide variety of behaviors and other physiological functions.

1. Introduction

The hormone prolactin (PRL) has been linked to over 300 functions in mammals, including water and electrolyte balance, growth and development, metabolism, and behavior (reviewed in Bole-Feysot et al., 1998). In birds and other vertebrates PRL also has many diverse functions ranging from feathering rate (Derks et al., 2018), reproduction (reviewed in Whittington and Wilson, 2013), stress modulation (reviewed in Angelier and Chastel, 2009), and parental behavior (reviewed in Smiley, 2019). PRL actions are mediated through the PRL receptor (PRLR) which is a membrane-bound receptor that is part of the class 1 cytokine receptor superfamily. As expected, PRLRs are found in a diverse range of tissues ranging from skin, bone tissue, liver, pancreas, kidney, and reproductive organs, among many others (see Bole-Feysot et al., 1998). In chicken and turkeys, PRL mRNA is found in peripheral tissues such the skin, kidney, and adrenal glands, which is consistent with PRL's role in osmoregulation, brood patch formation, and molting (reviewed in Ohkubo, 2017). With respect to PRL's role in behavior, PRLRs are found throughout the central nervous system (CNS) including hypothalamic sites, cortex, hippocampus, choroid plexus, and striatum in mammals (Bole-Feysot et al., 1998). Central specific binding sites for PRL have been detected in pigeons (*Columba livia domestica*), Wilson's phalarope (*Phalaropus tricolor*), dark-eyed juncos (*Junco hyemalis*), chickens, and turkeys (Ohkubo et al., 1998a, 1998b; Smiley, 2019; Zhou et al., 1996), although, to date, a detailed mapping of PRLRs is most complete in the ring dove (*Streptopelia risoria*; Buntin, et al., 1993; Fechner and Buntin, 1989). In ring doves, the highest concentrations of PRLRs for both males and females were found in hypothalamic nuclei,

* Corresponding author.
E-mail address: kos24@cornell.edu (K.O. Smiley).
[1] Current address: Centre for Neuroendocrinology and Department of Anatomy, School of Biomedical Sciences, University of Otago, Dunedin 9016, New Zealand.

https://doi.org/10.1016/j.ygcen.2020.113657
Received 22 June 2020; Received in revised form 29 October 2020; Accepted 31 October 2020
Available online 5 November 2020

including the preoptic area, lateral hypothalamus, tuberal nucleus, ventromedial hypothalamus, and paraventricular nucleus, as well as several extrahypothalamic brain regions such as the lateral septum and nucleus accumbens (Buntin et al., 1993; Buntin and Ruzycki, 1987).

In birds, PRL plays a particularly strong role in promoting parental behaviors (see Smiley, 2019 for a review). However, most of these studies have only manipulated peripheral levels of PRL and very few have tested the hypothesis that these behavioral effects are mediated through central PRLRs. In ring doves, central injections of PRL induce parental behavior in males and females (reviewed in Buntin, 1996). Specifically, intracerebroventricular (ICV) injections of PRL to access the preoptic area, ventromedial hypothalamus, or tuberal nucleus stimulate regurgitation and hyperphagia (reviewed in Buntin, 1996). Ring dove males and females are unique to birds as they feed squabs by regurgitating crop milk which is produced by the epithelial mucosal cells along the wall of the crop sac in response to PRL, an evolved trait unique to pigeons and doves (Buntin, 1996; Patel, 1936). However, ICV injections of PRL at levels that are too low to stimulate crop milk production in non-breeding ring doves still increase regurgitation feeding towards foster squabs (Buntin, 1996), suggesting central PRL action could also play a role in chick feeding in other birds. However, this remains a hypothesis until additional studies which manipulate central PRL/PRLR are performed. Testing this hypothesis in several different avian species with varying parental care systems is necessary in order to understand if PRL's role in avian parental care can be generalized across species. However, there is a considerable lack of information on the distribution of PRLRs in the avian CNS to test the hypothesis that parental care is mediated through central PRLRs in species that do not require the production of crop milk. In addition to parental care, this lack of information also prevents us from testing the role of PRL in other behaviors or functions and is necessary in order to proceed further in PRL related research in birds.

The PRLR distribution can be dynamic, however, and has been shown to be dependent on reproductive state in both mammals and birds. For example, PRLR mRNA concentrations in the anterior pituitary and basal hypothalamus increased and decreased, respectively, in incubating hens relative to laying or out-of-lay hens (Ohkubo et al., 1998a, 1998b). In mammals, PRLR mRNA in the olfactory bulb and hippocampus increased and decreased in diestrus and lactating females, respectively (de Moura et al., 2015). Additionally, hypothalamic PRLR immunoreactivity (ir) increased in lactating rats, compared to those in diestrus (Pi and Grattan, 1999). These results suggest that the CNS becomes increasingly or decreasingly sensitive to PRL's actions, in localized regions, depending on the animal's reproductive or behavioral state.

Activation of the PRLR leads to a cascade of intracellular events. Similar to mammals, when PRL is coupled with the PRLR in birds, it phosphorylates Janus kinase 2 (JAK2), which, in turn, phosphorylates the signal transducer and activator of transcription 5 (STAT5) resulting in signal transduction in the nucleus (Ohkubo, 2017). Phosphorylated STAT5 (pSTAT5)-ir activity in the brain varies depending on reproductive state, with higher pSTAT5-ir activity in the preoptic area, suprachiasmatic nucleus, lateral hypothalamus, ventromedial hypothalamus, paraventricular nucleus, lateral bed nucleus of the stria terminalis, and lateral septum during the late incubation stage of ring doves, when circulating PRL is highest relative to non-breeding doves (Buntin and Buntin, 2014). Indeed, peripheral injections of PRL alone increase pSTAT5-ir in these same areas (Buntin and Buntin, 2014), also indicating that circulating PRL actions can influence CNS PRLR activity. Although the JAK/STAT pathway can be activated in multiple cytokine signaling pathways (Aaronson and Horvath, 2002), STAT5 is most prominently activated downstream of the PRLR and provides a reliable readout of PRL signal transduction (Brown et al., 2010; Gouilleux et al., 1994; Lerant et al., 2001). Therefore, it has been commonly used as a marker for recent neural PRLR activity. In both rodents and ring doves there is a strong overlap between the PRLR distribution and pSTAT5 activity (Brown et al., 2010; Buntin and Buntin, 2014; Buntin et al., 1993; Pi and Grattan, 1998), further supporting that pSTAT5 can be used as a proxy for PRLR activation.

In order to advance the research on PRL and PRLR activity in the avian CNS, we collected brains from breeding and non-breeding zebra finches and subjected them to two different immunohistochemical (IHC) protocols. For the first IHC, we used an antibody which detected the PRLR to describe the distribution of PRLR throughout the zebra finch brain. We then compared brains from breeding and non-breeding birds to test if the PRLR distribution was dependent on breeding state. Next, we stained a series of tissues from the same brains for pSTAT5 to measure PRLR activity during breeding and non-breeding times. Examining pSTAT5 activity can help elucidate potential targets for studying behavior and PRL's other functions more generally. Together, this study provides the first description of PRLR and pSTAT5 activity in a songbird and is an essential first step before manipulation studies of PRLR can be performed.

2. Methods

2.1. Subjects

This study used 12 adult zebra finches (N = 6 breeding and N = 6 non-breeding, 3 males/3 females in each group) of mixed reproductive experience levels raised in the lab. Subjects were randomly assigned to be breeding or non-breeding. Breeding birds were housed only with their partner until their chicks were two days old post-hatch, when circulating PRL is found to be highest (Smiley and Adkins-Regan, 2016a, 2016b). Non-breeding subjects were non-paired birds that were housed in single-sex cages prior to brain collection. We chose to use non-paired birds as a control because in this species paired birds begin to breed very quickly under lab conditions, and therefore we wanted to eliminate any potential changes that are associated with breeding that co-occur with pairing.

All birds had access to food (commercial seed mix; Kaytee Fortifinch Diet), water, and grit *ad libitum*. Birds were supplemented with hard-boiled egg once per week. All rooms were kept in temperature (22.2° C) and humidity (range 30–70%) controlled rooms on 14:10 light:dark cycles. Male-female breeding pairs were housed in small breeding cages (0.6 m × 0.4 m × 0.35 m) that contained a nest box and nesting material (coconut fibers) available *ad libitum*. Daily nest checks were performed to monitor each pair's breeding status. Non-breeding birds were housed in single-sex aviaries (0.94 m × 0.76 m × 0.94 m) that held up to 20 birds. All methods and procedures were approved by the Cornell University IACUC.

2.2. Brain collection and sectioning procedures

Brains from breeding and non-breeding birds were collected on the same day. Birds were euthanized by an overdose of isoflurane vapor and perfused transcranially with phosphate-buffered solution followed by 4% paraformaldehyde (as in Kelly and Goodson, 2014). Brains were removed and post-fixed in 4% paraformaldehyde overnight before they were transferred to 70% ethyl alcohol. Brains were then embedded into a paraffin block and sectioned at 6 μm, taking every other section. Slides were divided into four series. One series (every 4th section) was stained for PRLR using immunohistochemistry (see Section 2.3) and another series was used for pSTAT5 IHC (see Section 2.5). Individual IDs were lost during tissue processing; therefore, sex differences could not be assessed. However, all breeding brain sections were mounted together on one set of slides and all non-breeding sections were mounted together on another set, so breeding treatment groups could still be evaluated. Based on prior work on parental behavior and PRL in this species (Smiley and Adkins-Regan, 2016a, 2016b, 2018a, 2018b), no sex differences were predicted *a priori*.

Note that while circulating PRL increases from anaesthesia in rats

Table 1
Antibody information.

Antibody (isotype)	Clonality	Host	Manufacturer	Immunogen	Dilution used
Anti-dove prolactin receptor antiserum	polyclonal	rabbit	ABR Affinity Bioreagents	cytoplasmic domain of the dove PRL receptor (see Table 2 for sequence)	1:3000
Anti-phospho-Stat5 (Tyr694)	polyclonal	rabbit	Cell Signaling Technology #9351, lot#6	synthetic phosphopeptide corresponding to residues surrounding Tyr694 of mouse Stat5a (amino acid sequence AVDGyVKPQC, where y _ phosphorylated tyrosine)	1:50 (1.56 μg/mL)

Table 2
Gene sequence for cytoplasmic domain of the ring dove (*Streptopelia risoria*) prolactin receptor. (a) Gene sequence of the dove prolactin receptor. (b) Translation of sequence in brackets from base # 29 - #1315 (=1287 base pairs) and is 429 amino acids. The antiserum was generated against two 17 amino acid chains within this sequence.

(a)

ATGAAGCAGA AATTGAGATC ATCAGTTCAA ATTATTTTGC TATTTGCTCT GATGGCAGTG 60
GGTTTGACTG GTCAATCATA CCCTGGAAAA CCTAAGATAA TAAGATGTCG TTCTCTAGAA 120
AAGGAAACCT TTTCTTGTTG GTGGAAGCCT GGCTCAGATG GAGGACTTCC TACCAATTAC 180
ACCCTGTTCT ACAGCAAGGA CAGTGAAGAA AAAATCTACG AATGTCCAGA CTATGGAATG 240
TCAGGTCCCA ATTCCTGCTA CTTCGATAAA AACCACACTA ATCCCTGGAC AACATATAAT 300
ATCACTGTAA TGGCAATGAA TGAGATTGGA AGTAACAGCT CAGATCCTCA GTATGTGGAT 360
GTGACCTCCA TAGTTCAGCC AGATGCTCCT GTGAACCTCT CTCTAGAAAC AAAAACATCT 420
GCTAGCACAA CGTGCCTTCT GGCAAAATGG TCTCCACCTC CAGTAGCTGA TGTCACCTCT 480
AATTCACATG TATATCGCTA TGAGCTACGA CTAAAACCTG AGGAAAAGGA AGAATGGGAG 540
ACAGTATCTG TTGGAGTACA GACACAGTAC AAAGTGAATA GGTTACAAGC TGGGGTGAAA 600
TATGTTGTTC AGGTCCGTTG TGTGCTAGAC GTTGGAGAAT GGAGTGAGTG GAGCTCTGAA 660
AGACACATTC ATATCCCCAA TGGAGAGTCA CCTCCTGAAA AGCCTACAAT AATAAAATGT 720
CGTTCTCCAG AAAAGGAAAC ATTTACTTGT TGGTGGAAAC CTGGTTCAGA TGGAGGACAT 780
CCTACTAACT ACACTTTGCT TTACAGCAAA GAAGGAGAGG AGCGAGTTTA TGAATGTCCA 840
GATTACAAAA CTGCAGGCCC CAATTCATGC TACTTCGATA AAAAGCACAC CTCTTTCTGG 900
ACCATATACA ATATAACTGT GAAGGCAACT AATGAAATTG GAAGTAATGT CTCTGATCCT 960
CTTTATGTGG ATGTGACTTA CATAGTACAG ACAGATCCTC CTGTTAATGT AACTCTGGAA 1020
TTAAAAAAGA CAGTCAATAG AAAACCATAT CTGGTCTTGA CATGGTCTCC ACCCCCGTTG 1080
GCTGATGTCA GATCTGGATG GCTTACACTT GATTATGAGT TACGACTAAA GCCTGAAGAA 1140
GCAGAGGAAT GGGAGACTAT TTTTGTTGGA CAGCAAACAC ATTATAAAAT GTTTAGTTTA 1200
AATCCCGGAA AGAAGTACAT TGTGCAGATT CACTGCAAAC CAGACCACCA TGGATCATGG 1260
AGTGAATGGA GCTTAGAAAA GTATATTCAG ATCCCTACTG ACTTTAGAAT AAAAGATATG 1320
GTTGTGTGGA TCATCGTCGG TGTCTTGTCA TCTCTTATAT GTTTAGTCAT GAGCTGGACA 1380
ATGGTTTTGA AAGGGTACAG AATGATAGCC TTTATCCTAC CACCAGTTCC GGGACCGAAG 1440
ATAAAAGGCA TAGATACACA TCTGTTAGAG ACAGGAAAAT CTGAAGAATT ATTGAGTGCT 1500
CTCGGTTGCC ATGGTTTCCC TCCAACATCA GACTGTGAAG AACTACTGAT AGAATATCTG 1560
GAGGTAGAGG ACAGTGAAGA TCAGCAACTC ATGCCAAGCC ATGACAATGG TCATCCCAAT 1620
AAAAATGCAA AAATGATAGC CAAGGAGACA GACAGTGACT CAGGCCGAGG AAGCTGTGAT 1680
AGCCCTTCTC TGCTTTCTGA GAAGTGCAGG GAGTCCCGTG CCATTCTATC AACACTTCAA 1740
ACCCAAGACA TAAGAGATGT TCAAGAAAAT AATGGAGGAA GGCACTGGGA AACTCAGTGT 1800
ATAGCCTCAG AACAGAAAAT ACTCCTTTTT AACAATGAGA GTACAAAATC GCCCATATGG 1860
CCTGCAGCTC AGTTACCTGA TAATCAGCCT CCTATGTTTG CCTACCACAG TACTGTAGAT 1920
GCGCACAAGA TAACACTGTG TACCATAGAT GTGAACATTG CACCAGTTTT GGTGGAAAAT 1980
GAAGAACAGC ATCAGCCACA ATATCCTATC ACTGAAACTG TCCACGACAA CATGGAAAAG 2040
CACAGAGAAA TGGAGAATTT GTATTCCAAA ACTGACCAAA CCACAGTGCA GGTCAAACAA 2100
AACAGACTTA ATGACAAGTC ACCTTTTTTG AAGCCTAAAC TAATGGATTA TGTAGAAGTT 2160
CACAAAGTCA GACAAGATGA GGTGCCAGCA GTATTACTGA AACATAAAGA AAATAGTGGA 2220
AAAATTGAAA AATACACTGT TCCAGGAACC AGCAAAGAAT ATACCAAGGT CTCAACTGTT 2280
GTGGACCATA ATATTCTGGT ATTAATGCCA GATTCACG

(b)

MKQKLRSSVQIILLFALMAVGLTGQSYPGKPKIIRCRSLEKETFSCWWKPGSDGGLPTNY 60
TLFYSKDSEEKIYECPDYGMSGPNSCYFDKNHTNPWTTYNITVMAMNEIGSNSSDPQYVD 120
VTSIVQPDAPVNLSLETKTSASTTCLLAKWSPPPVADVTSNSHVYRYELRLKPEEKEEWE 180
TVSVGVQTQYKVNRLQAGVKYVVQVRCVLDVGEWSEWSSERHIHIPNGESPPEKPTIIKC 240
RSPEKETFTCWWKPGSDGGHPTNYTLLYSKEGEERVYECPDYKTAGPNSCYFDKKHTSFW 300
TIYNITVKATNEIGSNVSDPLYVDVTYIVQTDPPVNVTLELKKTVNRKPYLVLTWSPPPL 360
ADVRSGWLTLDYELRLKPEEAEEWETIFVGQQTHYKMFSLNPGKKYIVQIHCKPDHHGSW 420
SEWSLEKYIQIPTDFRIKDMVVWIIVGVLSSLICLVMSWTMVLKGYRMIAFILPPVPGPK 480
[IKGIDTHLLETGKSEELLSALGCHGFPPTSDCEELLIEYLEVEDSEDQQLMPSHDNGHPN 540
KNAKMIAKETDSDSGRGSCDSPSLLSEKCRESRAILSTLQTQDIRDVQENNGGRHWETQC 600
IASEQKILLFNNESTKSPIWPAAQLPDNQPPMFAYHSTVDAHKITLCTIDVNIAPVLVEN 660
EEQHQPQYPITETVHDNMEKHREMENLYSKTDQTTV]QVKQNRLNDKSPFLKPKLMDYVEV 720
HKVRQDEVPAVLLKHKENSGKIEKYTVPGTSKEYTKVSTVVDHNILVLMPDS 772

(Isherwood and Cross, 1980), Harvey et al., (1978) found no significant differences in plasma PRL in chickens while under anaesthesia. We did not measure plasma PRL in our subjects, and are unaware of any study that has measured plasma PRL in zebra finches while under anaesthesia, but the time of handling and time spent under anaesthesia prior to perfusion is quite short (<5 min) and so we would not expect this manipulation to significantly alter PRLR or pSTAT5 expression levels centrally.

2.3. PRLR immunohistochemistry

After deparaffinization in xylene and rehydration in graded ethanol, sections were subjected to antigen retrieval by steaming in citrate buffer (10 mM, pH = 6.0). The endogenous peroxidase activity was quenched

by 0.3% hydrogen peroxide in distilled water for 10 min. Non-specific staining was blocked with a mixture of 10% goat serum and 2X casein for 30 min at room temperature. The primary antibody, rabbit polyclonal anti-dove prolactin receptor serum (Table 1) was used at 1:3,000 and incubated for 1.5 hr at room temperature. After washing, the sections were further incubated with biotinylated goat anti-rabbit IgG (10 ug/mL, Jackson ImmunoResearch Laboratories, Inc.) for 30 min and followed by streptavidin-horseradish peroxidase (Ready to Use, Vector Laboratories) for 15 min at room temperature. Negative controls were run in parallel by replacing the primary antibody with rabbit serum at the same dilution. For easy handling and minimizing variations across all samples, slides of multiple cases were loaded into MicroProbe System (Fisher Scientific) and PBST (0.05% Tween 20) was used for washing throughout the procedure. Nova Red (Vector Laboratories) was used as chromogen to visualize antigen localization, and the sections were lightly counterstained with hematoxylin. IHC results were examined by Olympus AX 70 compound microscope equipped with MicroFire camera and PictureFrame for image processing and capture (Optronics).

2.4. PRLR antibody generation

The rabbit polyclonal antibody used in PRLR immunohistochemistry was generated by ABR Affinity Bioreagents, Inc (Golden, Co; now Thermo-Fisher Scientific, Waltham, MA). The antiserum was generated against two 17 amino acid sequences in the cytoplasmic domain of the ring dove (*Streptopelia risoria*) prolactin receptor, which was cloned and sequenced by one of the coauthors (S.R.; Table 2). The IgG fraction of the antiserum was isolated by ammonium sulfate precipitation and further purified using epitope-specific affinity chromatography using a multi-step gradient elution process. Antibody purity was further verified with ELISA and SDS-PAGE. In immunohistochemistry assays, negative controls were run in parallel by replacing the PRLR with non-immune rabbit IgG at the same dilution. No specific staining was observed in these sections. Earlier validation tests revealed that this antibody yielded regional staining patterns in dove brain tissue that were virtually identical to those obtained using a previously validated rabbit polyclonal antiserum generated against the chicken prolactin receptor by Dr. Peter Sharp (Roslin Institute, University of Edinburgh).

2.5. pSTAT5 immunohistochemistry

Following deparaffinization in xylene and rehydration in graded ethanol, the sections were subjected to antigen retrieval by steaming in citrate buffer (10 mM, pH = 6.0) for 20 min followed by cooling down at room temperature for 30 min. The endogenous peroxidase activity was quenched by 0.3% hydrogen peroxide in distilled water for 10 min. IHC staining was performed by using ImmPRESS HRP Anti-Rabbit Ig (Peroxidase) Polymer Detection Kit (Vector Laboratories) following the kit instructions. The tissue section was incubated with rabbit anti-phospho-STAT5 (Tyr694) (Cell Signaling Technology, Cat#935, lot#6, RRID:AB_2315225) (Buntin and Buntin 2014) at 1:50 (1.56 ug/mL) for 1.5 hr at room temp (Table 1). The Phospho-STAT5 (Tyr694) antibody is specific for the phosphorylated protein, but does not distinguish between phosphoSTAT5a and phosphoSTAT5b. This antibody detects endogenous levels of STAT5a only when phosphorylated at Tyr694 and STAT5b when phosphorylated at Tyr699 and does not cross-react with the corresponding phospho-tyrosine residues of other STAT proteins (manufacturer's technical information). Antibodies were purified by protein A and peptide affinity chromatography and stains a single band of 90 kD molecular weight on Western blot (manufacturer's technical information). The PRLR activates the same JAK-STAT pathway in birds, as it does in mammals, (Ohkubo, 2017) and has successfully been used to detect pSTAT5 activity in ring doves (Buntin and Buntin 2014). Negative controls, washing, chromogen staining, and visualization were conducted as above (Section 2.3).

Table 3
Color parameters used for quantification for PRLR and pSTAT5 staining using the Aperio Positive Pixel Count Algorithm. Refer to Fig. 1c for a visual depiction of the color wheel used to generate values for hue value, hue width, and saturation. See Fig. 1d for a visual schematic of how intensity values were generated.

Color Parameters	PRLR	pSTAT5	Definition (from manufacture's user guide)
Hue value	0.9	0.9	This is the hue position on the color wheel used for positive staining (See Fig. 1c). Each hue on the circle has a number assigned to it, ranging from 0 to 1; Red = 0.0, Green = 0.33, Blue = 0.66.
Hue width	0.201	0.157	This value selects the range of hues, centered on the Hue Value, that will satisfy the hue detection process (refer to Fig. 1c). The number can range between zero and 1, where zero is a narrow hue width and 1 selects the entire range of hues.
Color Saturation Threshold	0.04	0.04	This is the required saturation of the Positive color. RGB values are represented as gray + color. The value can be between 0.0 and 1.0, with 1.0 corresponding to no gray component (fully saturated). Pixels with saturation less than this value are not reported.
Intensity	–	–	The intensity limits establish three intensity ranges for classifying and summing positive pixel values. The measure of brightness of the pixel and is the average of R + G + B values of the pixel; the greater the intensity value, the brighter the pixel (see Fig. 1d). Intensity reflects grey scale values ranging from 0 (black) to 255 (bright white).
Intensity Threshold Negative Pixels/Intensity Threshold weak-positive (Upper Limit)	180	150	Upper limit of intensity for weak-positive pixels (Iwp). Iwp is also used as an intensity threshold for negative stained pixels (pixels which do not meet the hue/saturation limits, but have an intensity less than Iwp).
Intensity Threshold weak-positive (Lower Limit / Intensity Threshold medium-positive (Upper Limit)	150	125	Lower limit of intensity for weak-positive pixels, which equals the upper limit of intensity for -medium positive pixels.
Intensity Threshold medium-positive (Lower Limit) / Intensity Threshold strong-positive (Upper Limit)	100	100	Lower limit of intensity for medium-positive pixels, upper limit of intensity for strong-positive pixels.
Intensity Threshold strong-positive (Lower Limit)	0	0	Lower limit of intensity for strong-positive pixels.

2.6. Quantification of immunostaining

All stained PRLR and pSTAT5 slides were digitized using the Aperio CS2 Scanscope (Leica Biosystems) and analyzed using the Aperio ImageScope program (version 12.3.2.8013, Leica Biosystems) at 20X magnification. Image analysis was performed using the Aperio Positive Pixel Count Algorithm, following the instructions from the manufacture's User's Guide (https://htrc.uchicago.edu/Downloads/MAN-0024-Rev-F.PDF). This type of automatic quantification is a well-established method of quantifying immunostained sections (e.g., Brazdziute and Laurinavicius, 2011; García-Rojo et al., 2014; Pillai et al., 2016), allows

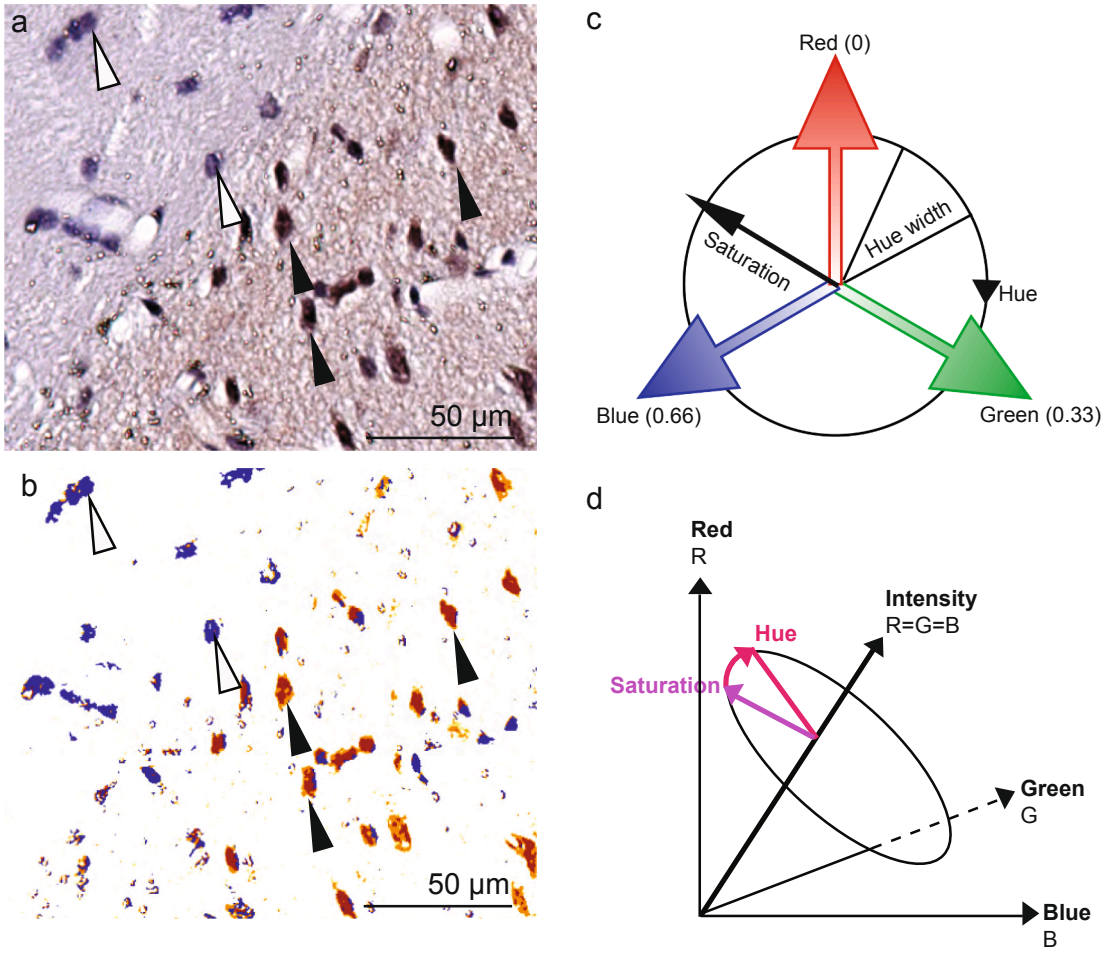

Fig. 1. Example of Positive Pixel Count Algorithm. (a) Original image stained for PRLR. (b) Markup image generated in ImageScope to verify color parameters. Blue = negative staining (counterstain only); red = strong positive staining; orange = medium positive staining; yellow = weak positive staining. Black arrows point to positive PRLR stained cells (a) and their corresponding algorithm detection (red, b), indicating only PRLR positive cells are marked as positive staining. White arrows point to H&E counterstained cells (a), and their corresponding algorithm detection (blue, b), indicating cells with only H&E staining are identified as negative staining. (c) Color wheel used to generate hue value, hue width, and saturation color parameters listed in Table 3. (d) Graphical depiction of how intensity values listed in Table 3 were generated.

for a greater number of sections of to be analyzed quickly, and greatly reduces human bias and potential counting errors as all images are analyzed under the same algorithm parameters, which are described below.

The Positive Pixel Count Algorithm quantifies the number of pixels in a defined region of interest based on user-specified color parameters (hue value, hue width, color saturation, and intensity – details and explanations of these parameters can be found in Table 3) which indicate positive staining (in this case, Nova red, which was used to visualize primary antibody staining). The positive staining is classified into three intensity ranges (weak, medium, and strong positive), as defined by the user (see Fig. 1 and Table 3). For the purposes of this analysis, the three ranges of positive staining were summed together to create one total positive pixel count for each section. In addition, pixels which are stained, but do not fall within the color parameters of the positive staining are also quantified, and these are referred to as 'negative' stained pixels (e.g., H&E counterstain only). When using the ImageScope program, a pseudo-color markup image is shown with an algorithm result (Fig. 1b). The markup image allows the user to confirm that the specified inputs are measuring the desired color and intensity ranges for positive and negative staining. Based on the comparison of the original and markup images, the user can further tune the color parameters to maximize the detection of positive and negative staining. Fig. 1 shows an example of the comparison of original (Fig. 1a) and markup images (Fig. 1b), suggesting the good agreement between manual scoring and automatic quantification analysis. Once a set of algorithm inputs has been confirmed, the settings can be saved as an algorithm macro for subsequent repeated use. For this study, the color parameters were set up for the PRLR and pSTAT5 staining separately by an independent investigator who was blind to treatment groups. The same algorithm was applied all sections analyzed for each respective set of immunostained slides. The color parameter settings used for the PRLR and pSTAT5 algorithm are listed in Table 3. In this report, the "positivity scores" refer to the proportion of positively-stained pixels to the total number of stained pixels (positive + negative). Brain regions were then classified into having 'high staining' (positivity score $\geq$ 0.6), 'medium staining' (positivity score between 0.3 and 0.6), or 'low staining' (positivity score between $\leq$ 0.3) or no staining (positivity score = 0).

The brain regions that were analyzed are listed in Table 4 and were identified using the canary (Stokes et al., 1974) and zebra finch (Nixdorf-Bergweiler et al., 2007) brain atlases, using the updated nomenclature from Reiner et al. (2004). The areas analyzed were chosen based on previous findings of the ring dove PRLR distribution (Buntin et al., 1993; Buntin and Ruzycki, 1987) and PRLR activation during post-hatch care (Buntin and Buntin, 2014), as well as several novel areas which have not been previously analyzed in other avian species, but were observed to have strong staining upon visual inspection. PRLR/pSTAT5 staining was analyzed in one hemisphere on the coronal section that

Table 4
Mean positivity scores for PRLR and pSTAT5 in breeding and non-breeding zebra finch brains. This table lists the brain regions examined and their abbreviations used throughout the paper. Mean positivity scores (proportion of total pixels that had positive staining in a given area for either PRLR or pSTAT5) and standard error of the mean (SEM) values across subjects are listed. PRLR and pSTAT5 staining was classified into having 'high staining' (pink boxes; positivity score ≥ 0.6), 'medium staining' (green boxes; positivity score between 0.3 and 0.6), or 'low staining' (yellow boxes; positivity score between ≤ 0.3). Statistical differences between breeders and non-breeders are reported for PRLR and pSTAT5 respectively. Significant differences ($p < 0.05$) are bolded.

		PRLR						PSTAT5					
		Breeder		Non-Breeder				Breeder		Non-Breeder			
Brain Area	Abbreviation	Mean positivity score	SEM	Mean positivity score	SEM	*U*	p-value	Mean positivity score	SEM	Mean positivity score	SEM	*U*	p-value
Nucleus accumbens	AC	0.61	14	0.74	5	6	0.41	0.52	25	0.23	6	4	0.39
Lateral part of the bed nucleus of the stria terminalis	BSTL	0.45	16	0.35	5	12	0.99	0.29	10	0.16	3	5	0.29
Medial part of the bed nucleus of the stria terminalis	BSTM	0.46	9	0.29	8	8	0.42	0.31	8	0.13	4	2.5	0.08
Cerebellum	CB	0.05	5	0.00	0	10	0.99	0.12	4	0.06	2	7	0.51
Choroid plexus	CHP	0.63	8	0.56	13	11	0.84	0.14	4	0.13	4	11	0.83
Lateral dorsal nucleus of thalamus	DLL	0.74	8	0.29	13	1	0.19	0.14	6	0.07	2	9	0.51
Medial dorsal nucleus of thalamus	DLM	0.52	18	0.22	15	3	0.20	0.10	4	0.06	2	6	0.41
Entopallium	E	0.37	10	0.33	7	12.5	0.99	0.12	6	0.12	3	10	0.65
Lateral geniculate nucleus	GLV	0.58	13	0.37	13	8	0.42	0.19	6	0.09	3	5	0.28
Globus pallidus	GP	0.47	11	0.32	10	8	0.42	0.20	10	0.21	4	10	0.65
Apical part of the hyperpallium	HA	0.61	11	0.77	8	8	0.42	0.14	4	0.64	13	0	**0.01**
Hippocampus	HP	0.63	12	0.64	11	11	0.84	0.14	4	0.35	10	5.5	0.17
HVC (formal name)	HVC	0.51	7	0.78	10	3	0.06	0.33	9	0.39	11	10	0.65
Nucleus isthmi, pars magnocellularis	IM	0.61	15	0.22	10	2	0.23	0.11	1	0.06	1	0.5	0.06
Tractus infundibularis	IN	0.87	5	0.42	16	1	0.11	0.39	14	0.37	13	6	0.99
Lateral hypothalamus	LHy	0.48	16	0.48	15	9	0.85	0.33	7	0.11	5	2	0.06
Lateral magnocellular nucleus of anterior nidopallium	LMAN	0.56	12	0.79	10	4	0.19	0.12	7	0.47	14	2	0.14
Mesopallium	M	0.66	3	0.77	6	5	0.15	0.18	6	0.49	6	0	**0.02**
Oculomotor nerve	N III	0.89	2	0.37	17	0	**0.03**	0.26	8	0.09	4	2	0.22
Nidopallium	N	0.50	9	0.56	7	9	0.55	0.11	3	0.41	7	1	**0.03**
Anterior preoptic area	POA	0.82	2	0.16	14	0	0.06	0.51	13	0.10	4	0	0.13
Medial preoptic area	POM	0.70	8	0.27	6	0	**0.04**	0.48	9	0.16	2	0	**0.04**
Nucleus preopticus paraventricularis magnocellularis	PPM	0.65	9	0.14	6	0	**0.02**	0.49	7	0.11	4	0	**0.04**
Paraventricular nucleus	PVN	0.61	12	0.43	7	9	0.55	0.34	9	0.19	4	7	0.31
Robust nucleus of arcopallium	RA	0.52	17	0.64	10	7	0.51	0.35	14	0.25	7	12	0.99
Nucleus rotundus	RT	0.49	11	0.47	6	11	0.84	0.13	7	0.08	1	10	0.69
Lateral septal nucleus	SL	0.60	14	0.32	12	5	0.15	0.17	4	0.21	7	10.5	0.74
Medial septal nucleus	SM	0.58	12	0.34	9	3	0.11	0.22	5	0.21	6	11	0.84
Lateral striatum	STL	0.54	9	0.26	12	4	0.10	0.18	10	0.18	5	10.5	0.73
Medial striatum	STM	0.57	10	0.55	14	12	0.99	0.11	1	0.22	8	3	0.25
Optic tectum	TEO	0.66	10	0.54	10	8	0.42	0.21	6	0.19	5	11	0.81
Nucleus taeniae of the amygdala	TnA	0.67	6	0.51	14	8	0.42	0.26	5	0.49	12	7	0.31
Tuberal nucleus	TU	0.85	5	0.17	9	0	**0.02**	0.48	12	0.43	18	6	0.79
Ventromedial hypothalamus	VMH	0.70	13	0.70	8	7	0.56	0.44	7	0.12	9	1	0.07
Ventral tegmental area or A10	VTA	0.70	14	0.65	5	4	0.19	0.39	7	0.13	2	0	**0.03**

displayed the largest extent of each brain area. Anatomical boundaries for each region were drawn based primarily on the canary brain atlas (Stokes et al., 1974). For two brains, one from each breeding group, the tissue was not usable due to poor perfusion, and thus were excluded from analysis, resulting in n = 5 for breeding and non-breeding brains.

2.7. Statistical analysis

Breeding and non-breeding differences in PRLR and pSTAT5 expression were assessed for each brain are separately using two-tailed Mann-Whitney U tests performed in Prism 8. Correlations between PRLR and pSTAT5 positivity scores were run for breeders and non-breeders separately using a Pearson's R test, controlling for bird ID, using SPSS version 25. For all tests, significance was accepted if $p < 0.05$.

3. Results

3.1. PRLR distribution and differences between breeders and non-breeders

We found that PRLRs are widely distributed throughout the brain (see Fig. 2 for entire distribution; example representative images of IHC staining for PRLR are in Fig. 4.). Overall, the sites with the greatest amount of immunoreactivity included the AC, POM, POA, PPM, CHP, M, HA, HP, TEO, VMH, PVN, TU, IN, DLL, IM, VTA, VMH, TnA, and NIII (See Table 4 for abbreviation definitions). Moderate PRLR staining was found in areas associated with visual processing such as the TEO, RT, E, GLV and IM and in areas related to song learning and production such as HVC, LMAN, and DLM. Little to no staining was observed in the CB. When comparing breeder and non-breeder data, the POM, PPM, TU, and NIII had greater PRLR expression in breeders, relative to non-breeders.

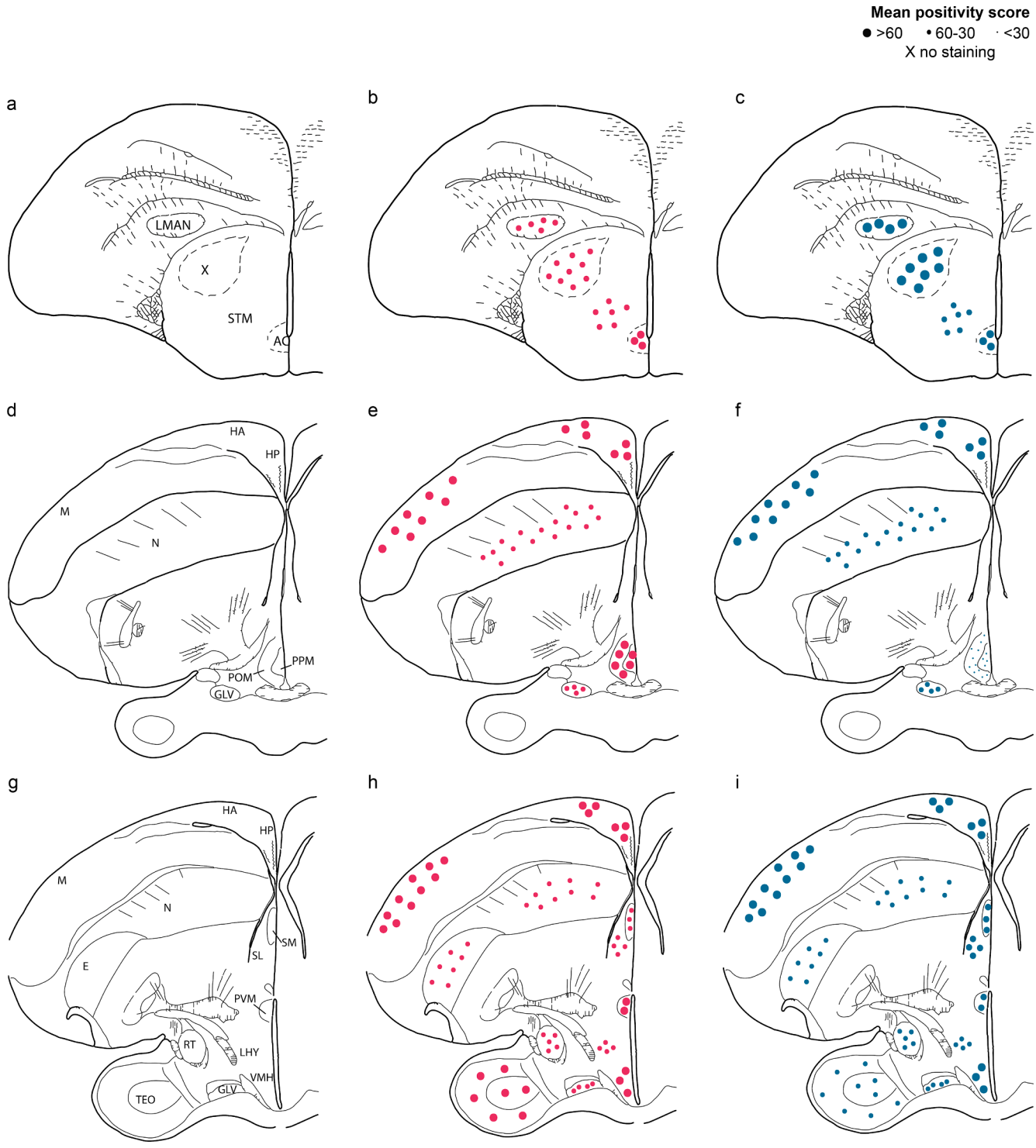

Fig. 2. PRLR distribution in breeding and non-breeding zebra finch brains. Figures on the far-left show brain areas which were analyzed; abbreviation names can be found on Table 4. Figures in the middle column (pink dots) depict the mean expression for breeders, whereas figures on the right depict the mean expression from non-breeders (teal dots). See Table 4 for mean positivity scores.

Mean positivity scores for PRLRs and statistics are reported in Table 4.

3.2. pSTAT5 distribution and differences between breeders and non-breeders

In general, pSTAT5 staining was at relatively low levels, with the exception of a few localized regions (see Fig. 3 for entire distribution; example representative images of IHC staining for pSTAT5 are in Fig. 4.). The regions with the greatest amount of pSTAT5 staining were the AC, POA, POM, PPM, VMH, TU, HA, LMAN, M, VTA, and TnA. However, the amount of pSTAT5 was primarily dictated by breeding status. Breeders showed more pSTAT5 immunoreactivity in the VTA, POM, and PPM, while non-breeders showed increased pSTAT5 immunoreactivity in the HA, M, and N. Mean positivity scores and statistics

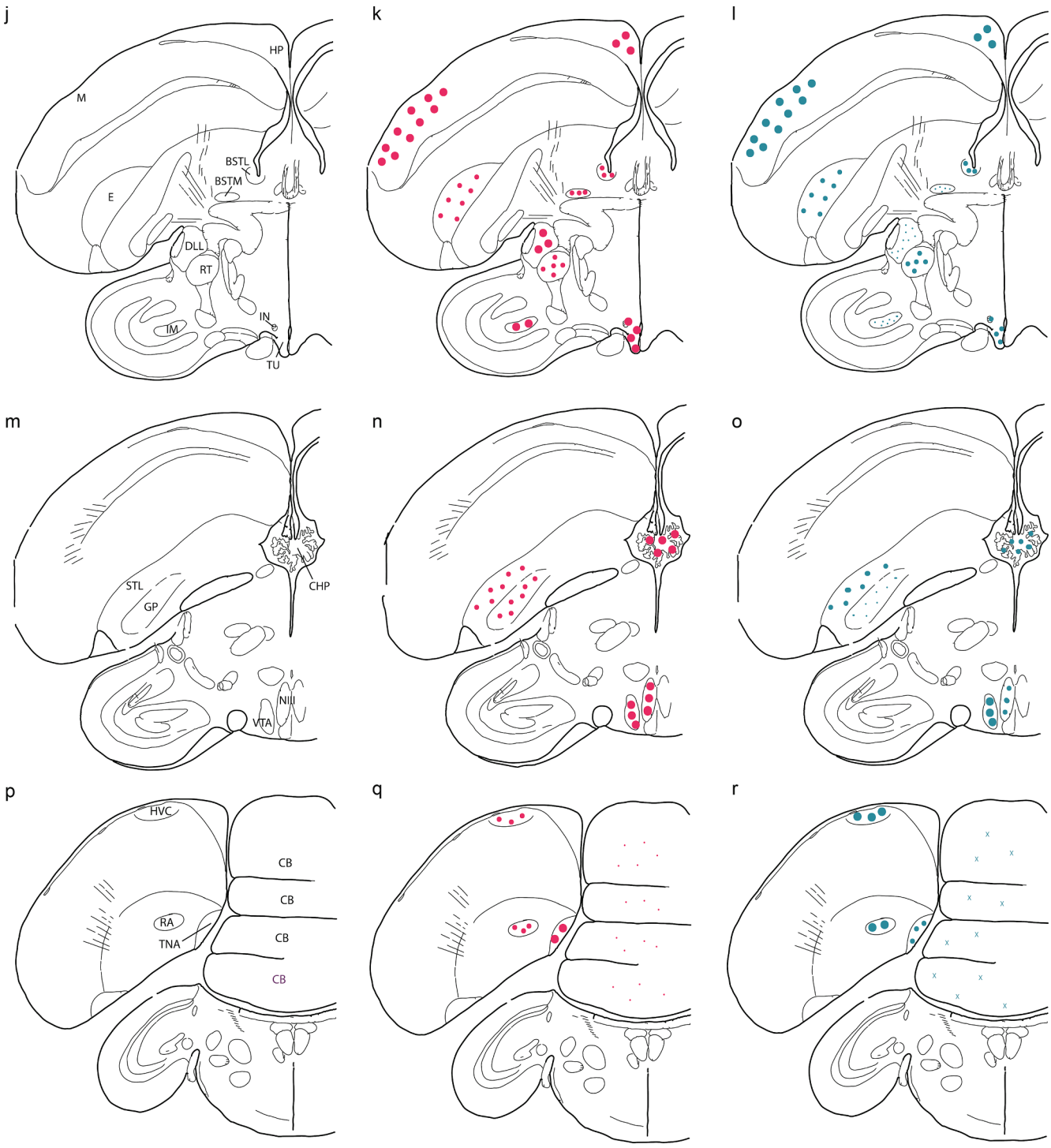

Fig. 2. (*continued*).

are reported in Table 4.

3.3. Positive correlations between PRLR and pSTAT5 expression in breeders and non-breeders

There was a significant positive correlation between breeders' PRLR and pSTAT5 positivity scores ($r(169) = 0.38$, $p < 0.01$) and between non-breeders' PRLR and pSTAT5 positivity scores ($r(168) = 0.41$, $p < 0.01$), which are shown in Fig. 5.

4. Discussion

4.1. Distribution of PRLR and pSTAT5 immunoreactivity

This is the first study to describe the PRLR and pSTAT5 distribution in a breeding and non-breeding songbird, the zebra finch. We found that PRLRs are widely distributed throughout the brain, exhibiting many similarities to ring doves and other birds (reviewed in Smiley, 2019). The most prevalent PRLR immunostaining was in the hypothalamus, which is consistent with other avian findings (reviewed in Smiley, 2019), as well as several mammalian and amphibian species (Muccioli

Fig. 3. pSTAT5 distribution in breeding and non-breeding zebra finch brains. Figures on the far-left show brain areas which were analyzed; abbreviation names can be found on Table 4. Figures in the middle (purple dots) depict the mean expression for breeders, whereas figures on the right depict the mean expression from non-breeders (blue dots). See Table 4 for mean positivity scores.

et al., 1988). Overall, pSTAT5 staining was at relatively low levels, with the exception of several areas which show differential expression due to breeding status (discussed below in 4.2). The most novel findings in this study were that PRLRs are expressed in many non-hypothalamic regions, such as the tectofugal visual pathway, song system, reward and saliency processing areas, and some pallium sites. PRL has over 300 identified functions in mammals (Bole-Feysot et al., 1998), so it is perhaps no surprise that PRLRs are found in such a diverse range of brain regions.

4.2. PRLR and pSTAT5 differences between breeding and non-breeding birds

The most striking difference in PRLR expression was observed in the POM/PPM region, where breeders showed significantly higher PRLR

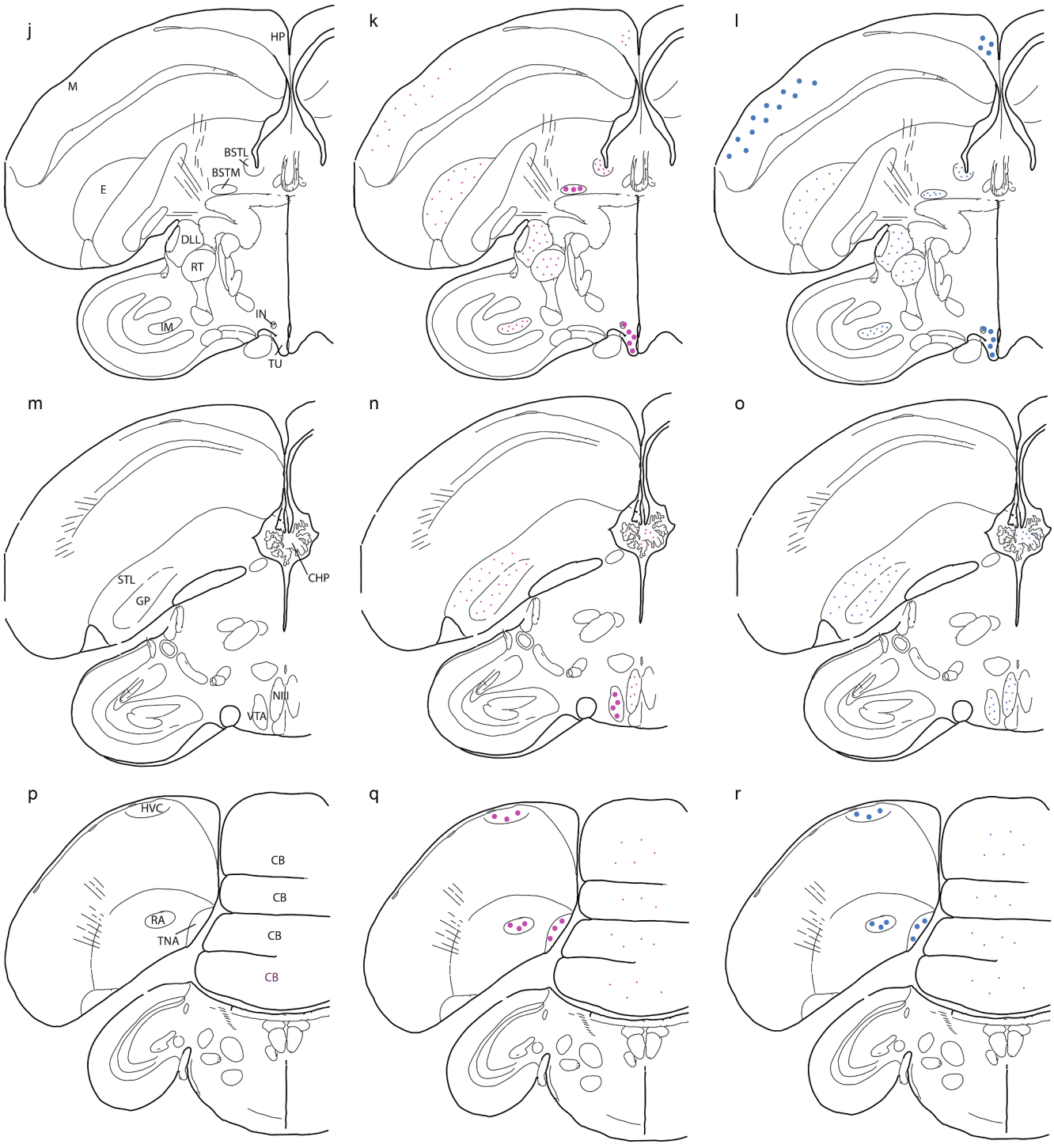

Fig. 3. (*continued*).

expression compared to non-breeders. The POM is a critical area for the expression of parental care in a variety of species and has been repeatedly reported to have a high density of PRLRs in both mammals (e.g., Kokay et al., 2006; Pi and Grattan, 1998) and birds (reviewed in Smiley, 2019). In ring doves, axon-sparing lesions of the POM decrease PRL-induced parental regurgitation feeding behavior (Slawski and Buntin, 1995) and microinjections of PRL into the POM increase food intake in non-breeding birds, which mimics the parental hyperphagia observed in parents provisioning their young (Hnasko and Buntin, 1993). Although PRL function in the POM has not been directly tested in zebra finches, given that altering circulating PRL levels significantly affects parental behavior (Smiley and Adkins-Regan, 2018a) and the PRLR distribution is similar to that of ring doves, suggests that PRL could be acting here to stimulate parental care in this species as well. This hypothesis is reinforced by the fact that the POM and PPM showed increased pSTAT5 staining in breeders that would be providing parental care compared to non-breeders. Direct manipulation of PRL and/or the PRLR in the POM in zebra finches is needed, however, to determine whether PRL plays a causal role here in simulating parental behavior.

Another area that showed increased PRLR expression during breeding was the TU (avian homolog of the mammalian arcuate nucleus), which is involved in the control of the release of PRL from the

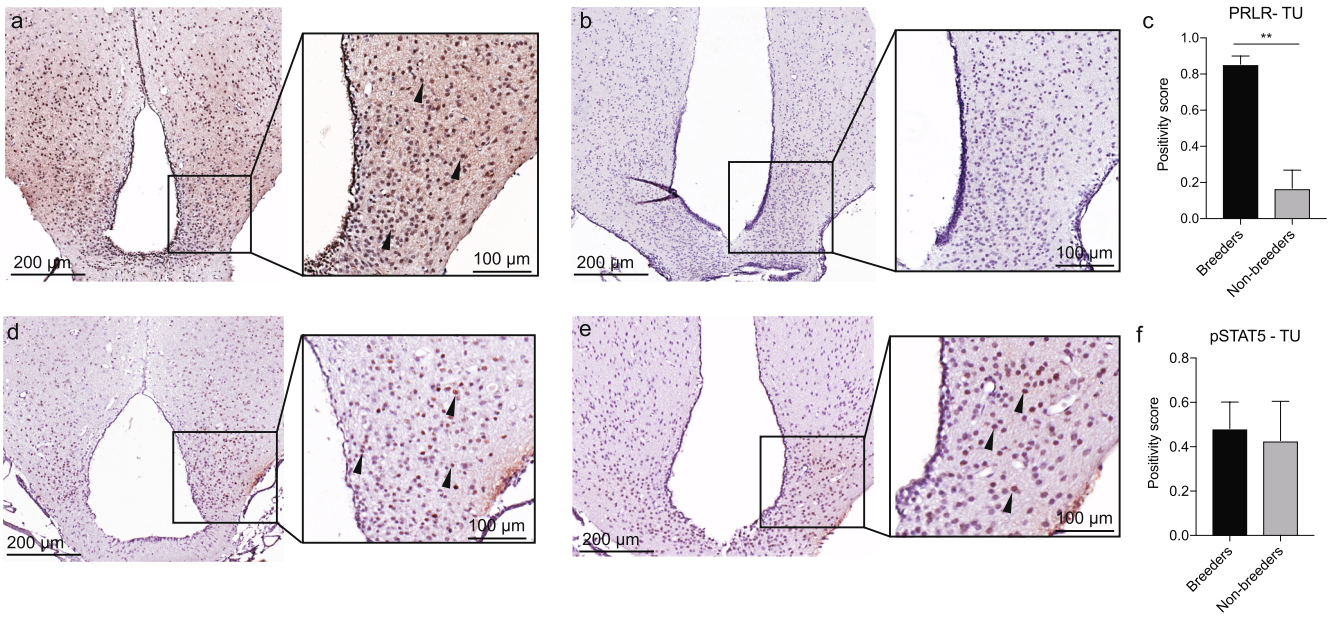

Fig. 4. Example representative images of IHC staining for PRLR and pSTAT5 used to generate Figs. 2 and 3. Arrows point to positivity stained cells for either PRLR (a, b insets) or pSTAT5 (d, e insets). (c) Quantification the mean positivity score ± SEM for PRLR staining and for (f) pSTAT5 staining, $^{**}p < 0.01$. Note the absence of PRLR staining in non-breeders (b), compared to breeders (a), while pSTAT5 staining patterns are nearly identical for breeders (d) and non-breeders (e).

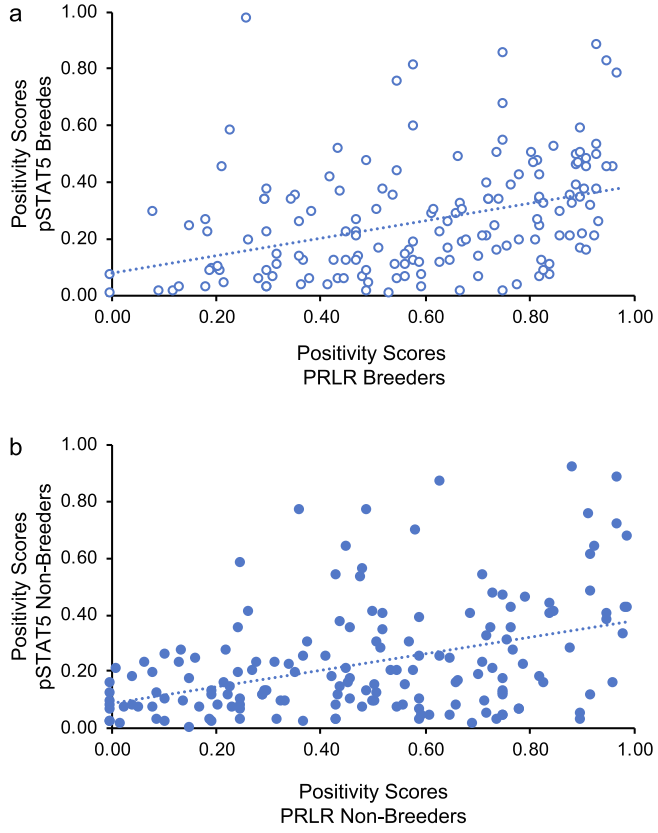

Fig. 5. Correlations between PRLR and PSTAT5 staining for breeding and non-breeding zebra finches. There were significant positive correlations between the mean PRLR and pSTAT5 positivity scores for (a) breeders (open dots) and (b) non-breeders (closed dots). Each dot represents an individual's positivity score for PRLR and pSTAT5 score. All scores for all individuals and brain areas are plotted here.

pituitary. In birds, PRL is stimulated by vasoactive intestinal peptide (VIP) released from neurons in the TU/IN into the median eminence, which then acts upon VIP receptors on the lactotroph cells in the anterior pituitary gland to stimulate the synthesis and release of PRL into the circulation (Kahtane et al., 2003; Sharp et al., 1998; Xu et al., 1996). In chickens and turkeys, VIP cell counts are low during non-laying times and significantly increase during incubation when circulating PRL is highest (Kosonsiriluk et al., 2008), which mirrors the increase in PRLR that is observed. Given the plasticity of both the VIP cell distribution and the PRLR expression in these regions, one possibility worth investigating is that PRLRs in the TU are expressed on VIP-neurons. While this remains to be tested, this information could advance our knowledge on how the TU regulates PRL secretion.

Overall, pSTAT5 staining was at relatively low levels in non-breeders, with the exception of the HA, M, and N which showed increased pSTAT5 staining in non-breeders, suggesting PRL may have a role at these sites that is not related to breeding. These findings are difficult to interpret, however, as there is no information on what PRL could be doing at these sites in birds or other animals. Much more research is required to understand what, if any, role PRL may be having throughout the avian brain, both in and outside of times of parental care. Breeding birds, on the other hand, showed increased staining in the POM but not the TU during the post-hatch period, which agrees with Buntin and Buntin's (2014) findings in ring doves. However, in contrast to our results, Buntin and Buntin (2014) found significant increases in pSTAT5 in the LHy, BSTL, and SL in breeders, whereas we found no such differences. At present, it is unclear whether this is a species difference or due to some other unknown factors. Overall, however, pSTAT5 appears to be increasing in regions known to regulate parental care during breeding when circulating PRL is highest and birds are caring for young, making it a promising candidate for future study of avian parental care.

4.3. Methodological considerations

Some methodological details should be taken into consideration when interpreting these data. First, although the pSTAT5 has provided informative data as to which PRL-responsive neurons are likely to be more active during breeding and non-breeding times, the pSTAT5 data should not be interpreted in the same way as studies of immediate early

gene expression are (e.g., c-fos, ZENK). We did not measure behavior or put birds through a particular task before collecting brain tissue. Birds were simply removed from their cage (either a single-sex cage in the non-breeding condition or their pair cage with offspring in the breeding condition) before sacrifice. Therefore, we cannot say for sure what these changes in pSTAT5 are in response to *per se*; we can only say that these basal levels are reflective of the breeding state the animal was in. A more controlled study which examines whether pSTAT5 activity changes in response to specific stimuli such as chick exposure in breeders, or a specific task which is known to utilize PRLR-rich brain regions in non-breeders, will need to be conducted in order to say for sure which PRL-responsive neurons are involved in certain tasks.

Second, while PRL has been shown to activate multiple signalling pathways, the STAT5 pathway appears to be the primary pathway that is activated (Brown et al., 2010; Buntin and Buntin, 2014). Indeed, Buntin and Buntin (2014) showed that treating ring doves with PRL results in increased pSTAT5-ir activity in regions which express the PRLR, similar to results found in rodents (Brown et al., 2010). There were strong, positive correlations between PRLR and pSTAT5 labelling in this study (Fig. 5), indicating that there was high overlap between PRLR expressing regions and pSTAT5 staining, as predicted. Therefore, while we are likely capturing a significant portion of activated PRLRs, there could be others that were not detected from the pSTAT5 alone. In addition, phosphorylation of STAT5 could also be caused by activation of cytokine pathways from ligands other than PRL such as growth hormone (Bennett et al., 2005) or leptin (Gong et al., 2007; Mütze et al., 2007) in similar regions that also contain the PRLR (Furigo et al., 2017; Ramesh et al., 2000).

We found several differences between PRLR and pSTAT5 activity in breeding birds, relative to non-breeders. However, because non-breeders had not recently engaged in pairing and mating behavior, it is possible that some effects observed could have been a result of undergoing courtship, mating, and/or forming a pair-bond with another conspecific. We have no concrete hypotheses as to which differences may be a result of pairing/mating, but it is a consideration which should be kept in mind for future studies.

4.4. Conclusions

In sum, we have described the PRLR and pSTAT5 distribution in a breeding and non-breeding songbird. Although many of these brain regions with PRLR expression may appear to be seemingly unrelated, several of these regions which express PRLR are in areas which are important for parental care. For instance, the POM has been repeatedly implicated in regulating parental behavior across taxa. Both PRLR and pSTAT5 activity increases in the POM in breeders, suggesting it may be involved in zebra finch parental care as well. Other regions, such as the VMH and VTA, may also be important for chick feeding and reward, and show increased pSTAT5 staining in breeders, but it is unknown if PRL plays a significant role at these areas during zebra finch parental care. At present, many of the possible functions of PRL have not been assessed in birds. However, given the similar distribution patterns of PRLR in both mammals and birds, across many brain regions, it seems plausible that there are highly conserved functions of PRL that are mediated by common neural substrates. Manipulation of PRL and/or the PRLR in these regions is required to determine what, if any, causal role PRL may have there. Nonetheless, this study represents the essential first step to inform the design of future causative studies which manipulate PRLR-expressing neurons and test their role in a wide variety of behaviors and other physiological traits.

CRediT authorship contribution statement

Kristina O. Smiley: Conceptualization, Formal analysis, Investigation, Writing - original draft, Visualization, Funding acquisition. **Longying Dong:** Methodology, Validation. **Selvakumar Ramakrishnan:** Methodology. **Elizabeth Adkins-Regan:** Supervision, Funding acquisition, Writing - review & editing.

Acknowledgements

We are grateful for the staff at the Histology/Cytology Core Facility and the Immunopathology Research and Development Laboratory at Cornell University Veterinary College for their help and assistance with this project. We would also like to thank Dr. John Buntin for generously providing us with the PRLR antibody and for helpful advice. This work was funded by an NSF DDIG ISO-501336 (KOS and EAR) and NSF ISO-1146891 (EAR). The data that support the findings of this study are available from the corresponding author upon request.

References

Aaronson, D.S., Horvath, C.M., 2002. A road map for those who don't know JAK-STAT. Science 296 (5573), 1653–1655. https://doi.org/10.1126/science.1071545.

Angelier, F., Chastel, O., 2009. Stress, prolactin and parental investment in birds: a review. Gen. Comp. Endocrinol. 163 (1–2), 142–148. https://doi.org/10.1016/j.ygcen.2009.03.028.

Bennett, E., McGuinness, L., Gevers, E.F., Thomas, G.B., Robinson, I.C.F., Davey, H.W., Luckman, S.M., 2005. Hypothalamic STAT proteins: regulation of somatostatin neurones by growth hormone via STAT5b. J. Neuroendocrinol. 17 (3), 186–194. https://doi.org/10.1111/j.1365-2826.2005.01296.x.

Bole-Feysot, C., Goffin, V., Edery, M., Binart, N., Kelly, P.A., 1998. Prolactin (PRL) and its receptor: actions, signal transduction pathways and phenotypes observed in PRL receptor knockout mice. Endocr. Rev. 19 (3), 225–268. https://doi.org/10.1210/edrv.19.3.0334.

Brazdziute, E., Laurinavicius, A., 2011. Digital pathology evaluation of complement C4d component deposition in the kidney allograft biopsies is a useful tool to improve reproducibility of the scoring. Diagn. Pathol. 6 (Suppl 1), S5. https://doi.org/10.1186/1746-1596-6-S1-S5.

Brown, R.S.E., Kokay, I.C., Herbison, A.E., Grattan, D.R., 2010. Distribution of prolactin-responsive neurons in the mouse forebrain. J. Comp. Neurol. 518 (1), 92–102. https://doi.org/10.1002/cne.22208.

Buntin, J. D. (1996). Neural and Hormonal Control of Parental Behavior in Birds. In Jay S. Rosenblatt and Charles T. Snowdon (Ed.), Advances in the Study of Behavior: Vol. Volume 25 (pp. 161–213). Academic Press. http://www.sciencedirect.com/science/article/pii/S0065345408603332.

Buntin, J.D., Buntin, L., 2014. Increased STAT5 signaling in the ring dove brain in response to prolactin administration and spontaneous elevations in prolactin during the breeding cycle. Gen. Comp. Endocrinol. 200, 1–9. https://doi.org/10.1016/j.ygcen.2014.02.006.

Buntin, J.D., Ruzycki, E., 1987. Characteristics of prolactin binding sites in the brain of the ring dove (< i> Streptopelia risoria</i>). Gen. Comp. Endocrinol. 65 (2), 243–253.

Buntin, J.D., Ruzycki, E., Witebsky, J., 1993. Prolactin Receptors in dove brain: autoradiographic analysis of binding characteristics in discrete brain regions and accessibility to blood-borne prolactin. Neuroendocrinology 57 (4), 738–750. https://doi.org/10.1159/000126432.

de Moura, A.C., Lazzari, V.M., Becker, R.O., Gil, M.S., Ruthschilling, C.A., Agnes, G., Almeida, S., da Veiga, A.B.G., Lucion, A.B., Giovenardi, M., 2015. Gene expression in the CNS of lactating rats with different patterns of maternal behavior. Neurosci. Res. 99, 8–15. https://doi.org/10.1016/j.neures.2015.05.003.

Derks, M.F.L., Herrero-Medrano, J.M., Crooijmans, R.P.M.A., Vereijken, A., Long, J.A., Megens, H.-J., Groenen, M.A.M., 2018. Early and late feathering in turkey and chicken: same gene but different mutations. Genetics Select. Evolut. 50, 7. https://doi.org/10.1186/s12711-018-0380-3.

Fechner, J.H., Buntin, J.D., 1989. Localization of prolactin binding sites in ring dove brain by quantitative autoradiography. Brain Res. 487 (2), 245–254.

Furigo, I.C., Metzger, M., Teixeira, P.D.S., Soares, C.R.J., Donato, J., 2017. Distribution of growth hormone-responsive cells in the mouse brain. Brain Struct. Funct. 222 (1), 341–363. https://doi.org/10.1007/s00429-016-1221-1.

García-Rojo, M., Sánchez, J.R., de la Santa, E., Durán, E., Ruiz, J.L., Silva, A., Rubio, F.J., Rodríguez, A.M., Meléndez, B., González, L., López-Viedma, B., 2014. Automated image analysis in the study of lymphocyte subpopulation in eosinophilic oesophagitis. Diagn. Pathol. 9 (Suppl 1), S7. https://doi.org/10.1186/1746-1596-9-S1-S7.

Gong, Y., Ishida-Takahashi, R., Villanueva, E.C., Fingar, D.C., Münzberg, H., Myers, M. G., 2007. The long form of the leptin receptor regulates STAT5 and ribosomal protein S6 via alternate mechanisms. J. Biol. Chem. 282 (42), 31019–31027. https://doi.org/10.1074/jbc.M702838200.

Gouilleux, F., Wakao, H., Mundt, M., Groner, B., 1994. Prolactin induces phosphorylation of Tyr694 of Stat5 (MGF), a prerequisite for DNA binding and induction of transcription. EMBO J. 13 (18), 4361–4369.

Harvey, S., Scanes, C.G., Chadwick, A.C., Bolton, N.J., 1978. The effect of thyrotropin-releasing hormone (TRH) and somatostatin (GHRIH) on growth hormone and prolactin secretion in vitro and in vivo in the domestic fowl (Gallus domesticus). Neuroendocrinology 26 (4), 249–260. https://doi.org/10.1159/000122831.

Hnasko, R.M., Buntin, J.D., 1993. Functional mapping of neural sites mediating prolactin-induced hyperphagia in doves. Brain Res. 623 (2), 257–266. https://doi.org/10.1016/0006-8993(93)91436-V.

Isherwood, K.M., Cross, B.A., 1980. Effect of the suckling stimulus on secretion of prolactin and luteinizing hormone in conscious and anaesthetized rats. The Journal of Endocrinology 87 (3), 437–444. https://doi.org/10.1677/joe.0.0870437.

Kahtane, A.A., Chaiseha, Y., Halawani, M.E., 2003. Dopaminergic regulation of avian prolactin gene transcription. J. Mol. Endocrinol. 31 (1), 185–196. https://doi.org/10.1677/jme.0.0310185.

Kelly, A.M., Goodson, J.L., 2014. Hypothalamic oxytocin and vasopressin neurons exert sex-specific effects on pair bonding, gregariousness, and aggression in finches. Proc. Natl. Acad. Sci. 111 (16), 6069–6074. https://doi.org/10.1073/pnas.1322554111.

Kokay, I.C., Bull, P.M., Davis, R.L., Ludwig, M., Grattan, D.R., 2006. Expression of the long form of the prolactin receptor in magnocellular oxytocin neurons is associated with specific prolactin regulation of oxytocin neurons. Am. J. Physiol. – Regulat., Integrat. Comp. Physiol. 290 (5), R1216–R1225. https://doi.org/10.1152/ajpregu.00730.2005.

Kosonsiriluk, S., Sartsoongnoen, N., Chaiyachet, O., Prakobsaeng, N., Songserm, T., Rozenboim, I., Halawani, M.E., Chaiseha, Y., 2008. Vasoactive intestinal peptide and its role in continuous and seasonal reproduction in birds. Gen. Comp. Endocrinol. 159 (1), 88–97. https://doi.org/10.1016/j.ygcen.2008.07.024.

Lerant, A., Kanyicska, B., Freeman, M.E., 2001. Nuclear translocation of STAT5 and increased expression of Fos related antigens (FRAs) in hypothalamic dopaminergic neurons after prolactin administration. Brain Res. 904 (2), 259–269. https://doi.org/10.1016/s0006-8993(01)02470-2.

Muccioli, G., Bellussi, G., Ghé, C., Pagnini, G., Di Carlo, R., 1988. Regional distribution and species variation of prolactin binding sites in the brain. Gen. Comp. Endocrinol. 69 (3), 399–405.

Mütze, J., Roth, J., Gerstberger, R., Hübschle, T., 2007. Nuclear translocation of the transcription factor STAT5 in the rat brain after systemic leptin administration. Neurosci. Lett. 417 (3), 286–291. https://doi.org/10.1016/j.neulet.2007.02.074.

Nixdorf-Bergweiler, B. E., Bischof, H.-J., Nixdorf-Bergweiler, B. E., & Bischof, H.-J. (2007). A Stereotaxic Atlas Of The Brain Of The Zebra Finch, Taeniopygia Guttata. National Center for Biotechnology Information (US).

Ohkubo, T., Tanaka, M., Nakashima, K., Sharp, P.J., 1998a. Relationship between prolactin receptor mRNA in the anterior pituitary gland and hypothalamus and reproductive state in male and female bantams (Gallus domesticus). Gen. Comp. Endocrinol. 111 (2), 167–176. https://doi.org/10.1006/gcen.1998.7099.

Ohkubo, T., Tanaka, M., Nakashima, K., Talbot, R.T., Sharp, P.J., 1998b. Prolactin receptor gene expression in the brain and peripheral tissues in broody and nonbroody breeds of domestic hen. Gen. Comp. Endocrinol. 109 (1), 60–68. https://doi.org/10.1006/gcen.1997.7008.

Ohkubo, Takeshi. (2017). Neuroendocrine Control of Broodiness. In Avian Reproduction (pp. 151–171). Springer, Singapore. https://doi.org/10.1007/978-981-10-3975-1_10.

Pi, Grattan, 1999. Increased prolactin receptor immunoreactivity in the hypothalamus of lactating rats. J. Neuroendocrinol. 11 (9), 693–705. https://doi.org/10.1046/j.1365-2826.1999.00386.x.

Pi, X.J., Grattan, D.R., 1998. Distribution of prolactin receptor immunoreactivity in the brain of estrogen-treated, ovariectomized rats. J. Comp. Neurol. 394 (4), 462–474.

Pillai, S., Center, S.A., McDonough, S.P., Demarco, J., Pintar, J., Henderson, A.K., Cooper, J., Bolton, T., Sharpe, K., Hill, S., Benedict, A.G., Haviland, R., 2016. Ductal plate malformation in the liver of boxer dogs: clinical and histological features. Vet. Pathol. 53 (3), 602–613. https://doi.org/10.1177/0300985815610567.

Ramesh, R., Kuenzel, W.J., Buntin, J.D., Proudman, J.A., 2000. Identification of growth-hormone- and prolactin-containing neurons within the avian brain. Cell Tissue Res. 299 (3), 371–383.

Reiner, A., Perkel, D.J., Bruce, L.L., Butler, A.B., Csillag, A., Kuenzel, W., Medina, L., Paxinos, G., Shimizu, T., Striedter, G., Wild, M., Ball, G.F., Durand, S., Güntürkün, O., Lee, D.W., Mello, C.V., Powers, A., White, S.A., Hough, G., Avian Brain Nomenclature Forum, 2004. Revised nomenclature for avian telencephalon and some related brainstem nuclei. J. Comp. Neurol. 473 (3), 377–414. https://doi.org/10.1002/cne.20118.

Sharp, P.J., Dawson, A., Lea, R.W., 1998. Control of luteinizing hormone and prolactin secretion in birds. Comp. Biochem. Physiol. C: Pharmacol. Toxicol. Endocrinol. 119 (3), 275–282.

Slawski, B.A., Buntin, J.D., 1995. Preoptic area lesions disrupt prolactin-induced parental feeding behavior in ring doves. Horm. Behav. 29 (2), 248–266. https://doi.org/10.1006/hbeh.1995.1018.

Smiley, K.O., 2019. Prolactin and avian parental care: new insights and unanswered questions. Horm. Behav. https://doi.org/10.1016/j.yhbeh.2019.02.012.

Smiley, K.O., Adkins-Regan, E., 2016a. Relationship between prolactin, reproductive experience, and parental care in a biparental songbird, the zebra finch (Taeniopygia guttata). Gen. Comp. Endocrinol. 232, 17–24. https://doi.org/10.1016/j.ygcen.2015.11.012.

Smiley, K.O., Adkins-Regan, E., 2016b. Prolactin is related to individual differences in parental behavior and reproductive success in a biparental passerine, the zebra finch (Taeniopygia guttata). Gen. Comp. Endocrinol. 234, 88–94. https://doi.org/10.1016/j.ygcen.2016.03.006.

Smiley, K.O., Adkins-Regan, E., 2018a. Lowering prolactin reduces post-hatch parental care in male and female zebra finches (Taeniopygia guttata). Horm. Behav. 98, 103–114. https://doi.org/10.1016/j.yhbeh.2017.12.011.

Smiley, K.O., Adkins-Regan, E., 2018b. Factors that influence the onset of parental care in zebra finches: roles for egg stimuli and prolactin. Behav. Process. 153, 47–54. https://doi.org/10.1016/j.beproc.2018.05.002.

Stokes, T.M., Leonard, C.M., Nottebohm, F., 1974. The telencephalon, diencephalon, and mesencephalon of the canary, Serinus canaria, in stereotaxic coordinates. J. Comparative Neurol. 156 (3), 337–374.

Whittington, C.M., Wilson, A.B., 2013. The role of prolactin in fish reproduction. Gen. Comp. Endocrinol. 191, 123–136. https://doi.org/10.1016/j.ygcen.2013.05.027.

Xu, M., Proudman, J.A., Pitts, G. R., Wong, E. A., Foster, D. N., el Halawani, M.E., 1996. Vasoactive intestinal peptide stimulates prolactin mRNA expression in turkey pituitary cells: Effects of dopaminergic drugs. Proceedings of the Society for Experimental Biology and Medicine. Society for Experimental Biology and Medicine (New York, N.Y.), 212(1), 52–62.

Zhou, J.F., Zadworny, D., Guémené, D., Kuhnlein, U., 1996. Molecular cloning, tissue distribution, and expression of the prolactin receptor during various reproductive states in Meleagris gallopavo. Biol. Reprod. 55 (5), 1081–1090.